

## Article

# Spectroscopic Investigation of a Color Painting on an Ancient Wooden Architecture from the Taiping Heavenly Kingdom Prince Dai's Mansion in Jiangsu, China

Kezhu Han <sup>1</sup>, Hong Yang <sup>1,2</sup>, Gele Teri <sup>1</sup>, Shanshuang Hu <sup>1,3</sup>, Jiaxin Li <sup>1</sup>, Yanli Li <sup>1</sup>, Ersudai Ma <sup>1</sup>, Yuxiao Tian <sup>1</sup>, Peng Fu <sup>4,\*</sup>, Yujia Luo <sup>1,\*</sup>  and Yuhu Li <sup>1,\*</sup>

<sup>1</sup> Engineering Research Center of Historical Cultural Heritage Conservation, Ministry of Education, School of Materials Science and Engineering, Shaanxi Normal University, Xi'an 710119, China

<sup>2</sup> The Imperial Palace Museum, Beijing 100009, China

<sup>3</sup> The First Historical Archives of China, Beijing 100031, China

<sup>4</sup> Shaanxi Institute for the Preservation of Culture Heritage, Xi'an 710004, China

\* Correspondence: fupeng@snnu.edu.cn (P.F.); yujialuo@snnu.edu.cn (Y.L.); liyuhu@snnu.edu.cn (Y.L.)

**Abstract:** This research sheds light on the analysis of pigments and adhesives applied on a color painting on wooden architecture in Taiping Heavenly Kingdom Prince Dai's mansion, located in Changzhou, Jiangsu Province in China. Four samples were collected from the painting above the building beam in the mansion, and the samples were analyzed and identified using a series of techniques, including polarized light microscopy (PLM), scanning electron microscope coupled with an energy-dispersive X-ray spectroscopy (SEM-EDS), micro-Raman spectroscopy (m-RS) and Fourier-transform infrared spectroscopy (FTIR). The results indicate that the red, black, blue, and green pigments were identified to be cinnabar, ivory black, indigo, and phthalocyanine green, respectively. The green pigment was inferred to be a lately repainted pigment based on its production age, suggesting that this ancient building had been refurbished or repaired. Given the good stability and visual effect of this green pigment, it is suggested to be used in future conservation processes. The pyrolysis-gas chromatography/mass Spectrometry (Py-Gc/Ms) results indicate that glue containing protein was used as a binder for the pigment samples, and that walnut oil might have been applied to the wooden architecture as a primer before painting. Our findings can well inform curators and conservators of the selection of appropriate restoration materials if necessary, and also provide data support for conservation of similar ancient buildings in southern China.

**Keywords:** color painting; ancient wooden architecture; pigments; adhesives; building conservation



**Citation:** Han, K.; Yang, H.; Teri, G.; Hu, S.; Li, J.; Li, Y.; Ma, E.; Tian, Y.; Fu, P.; Luo, Y.; et al. Spectroscopic Investigation of a Color Painting on an Ancient Wooden Architecture from the Taiping Heavenly Kingdom Prince Dai's Mansion in Jiangsu, China. *Minerals* **2023**, *13*, 224. <https://doi.org/10.3390/min13020224>

Academic Editor: Daniela Pinto

Received: 12 January 2023

Revised: 29 January 2023

Accepted: 30 January 2023

Published: 3 February 2023



**Copyright:** © 2023 by the authors. Licensee MDPI, Basel, Switzerland. This article is an open access article distributed under the terms and conditions of the Creative Commons Attribution (CC BY) license (<https://creativecommons.org/licenses/by/4.0/>).

## 1. Introduction

Taiping Heavenly Kingdom Prince Dai's mansion is located in Jintan County, Changzhou, Jiangsu Province (Figure 1a,b). The mansion was built in around 1862 as the residence for Prince Dai, named Huang Chengzhong (1826–1865). He was one of leaders for the Taiping army during the rebellion that was waged in China between the Qing dynasty and the Taiping Heavenly Kingdom from 1851 to 1864. After the reform and opening up, the mansion was opened to visitors and has become a famous tourist attraction in Changzhou. There are a large number of paintings of great significance in the mansion, and, according to the site survey, the color paintings were directly executed on the wooden beams (Figure 1c).

Color painting, i.e., application of various pigments on ancient Chinese wooden architecture, is an important tangible heritage asset of historical, artistic, and cultural value. Such application can decorate wood texture and inhomogeneous wood color and can also prevent the wood from eroding as a result of an undesirable environment [1]. The use of pigments on wooden objects could be traced back as early as the Spring and Autumn period (approximately 770 to 476 BC). Various painting patterns were gradually invented

and adopted, such as motifs of dragons and clouds, as well as brocade patterns used in the Qin and Han dynasties. It is reported that repeated motifs of animals and iridescent clouds were discovered on the coffins in the Mawangdui Han Dynasty Tomb [2]. More painting styles were created in the Song dynasty, e.g., the stacked halo painting method. The development of painting styles and methods had not reached their peak until the Ming and Qing dynasties.

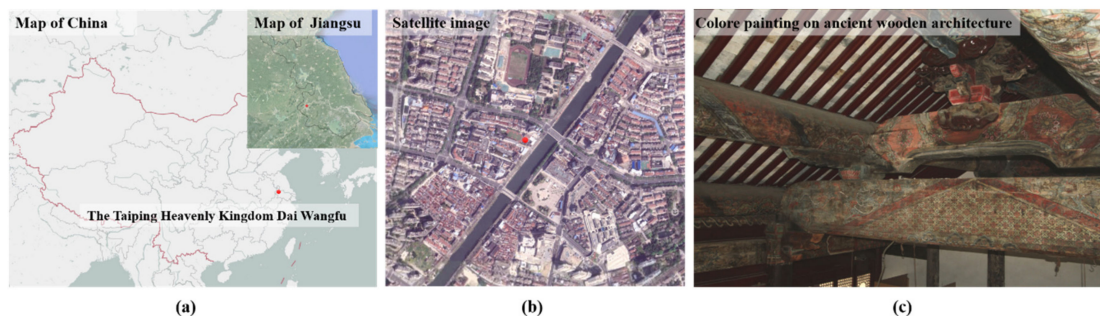


**Figure 1.** (a) The location of the Taiping Heavenly Kingdom Prince Dai's mansion (the red dot), situated in Jintan County, Changzhou, Jiangsu Province; (b) Satellite image of the location of Dai Taiping Heavenly Kingdom Prince Dai's mansion (The red dot represents the location of the mansion); (c) The color painting executed on the wooden beams in Taiping Heavenly Kingdom Prince Dai's mansion.

It is known that pigments are categorized into inorganic and organic pigments. Inorganic pigments refer to mineral substances, e.g., the most common red pigments include cinnabar ( $\text{HgS}$ ), hematite ( $\alpha\text{-Fe}_2\text{O}_3$ ), and red lead ( $\text{Pb}_3\text{O}_4$ ); common blue pigments include azurite [ $2\text{CuCO}_3\cdot\text{Cu}(\text{OH})_3$ ], ultramarine [ $(\text{Na,Ca})_8(\text{AlSiO}_4)_6(\text{SCl})_2$ ], and Chinese blue ( $\text{BaCuSi}_4\text{O}_{10}$ ); common green pigments include malachite [ $\text{CuCO}_3\cdot\text{Cu}(\text{OH})_2$ ], emerald [ $\text{Cu}(\text{CH}_3\text{COO})\cdot 3\text{Cu}(\text{AsO}_2)_2$ ], and atacamite [ $\text{Cu}_2(\text{OH})_3\text{Cl}$ ]; the most-used yellow pigments are orpiment ( $\text{As}_2\text{S}_3$ ) and realgar ( $\text{As}_4\text{S}_4$ ); common white pigments include lead white [ $2\text{PbCO}_3\cdot\text{Pb}(\text{OH})_2$ ] and chalk ( $\text{CaCO}_3$ ); and the most frequently used black pigments are graphite ( $\text{C}$ ) and iron black ( $\text{Fe}_3\text{O}_4$ ). The identified pigments on wooden architecture in China are summarized in Table 1. These mineral pigments were often used for paintings on buildings, artifacts of tombs, etc. For example, it has been found that cinnabar was used on artifacts in royal tombs at the Yinxu site, built in the late Shang dynasty as early as 1319–1046 BC [3], and Egyptian blue, yellow ochre, and red ochre were discovered on the Egyptian fresco of the Karnak temples (2040–1782 BC) [4]. The widespread use of the mineral pigments is due to their good stability and durability even in harsh environments such as high-humidity environments, e.g., tombs.

Organic pigments are generally derived from plants and marine animals, such as alizarin, orchids, and insects. Fuchsia, discovered by accident by William Henry Perkin during synthesis of quinine, is the first artificially synthesized dye. Indigo blue ( $\text{C}_{16}\text{H}_{10}\text{N}_2\text{O}_2$ ), a blue pigment extracted from orchids, is one of the most commonly used fabric dyes over time [5]. The synthesized phthalocyanine pigment in the early 20th century has greatly enriched the blue–green organic pigment variety [6]. Although natural organic dyes are bright, non-toxic, and affordable [7], they tend to be relatively unstable compared with the inorganic pigments, especially when exposed to light, fluctuating conditions, or an acidic or alkaline environment.

Pigments can be identified mainly from three perspectives: morphology observation, elements determination, and composition identification. Firstly, polarized light microscopy (PLM) [8] is used to observe pigment morphology, including particle sizes and optical properties, in order to distinguish artificial and natural mineral pigments, during which a small amount of samples is needed. Secondly, elements in pigments can be determined using methods such as scanning electron microscope coupled with an energy-dispersive X-ray spectroscopy (SEM-EDS) [9], energy-dispersive X-Ray spectroscopy (XRF) [10], Fourier-transform infrared spectroscopy (FT-IR) [11], and X-ray photoelectron spectroscopy

(XPS) [12]. Finally, X-ray diffraction (XRD) [13] and micro-Raman spectroscopy (m-RS) [14] are used to further identify crystalline structures and phase composition for pigments, and are non-destructive and highly sensitive. All these methods have been reported in several studies, as summarized in Table 1.

Organic adhesives are another important component to adhere the pigment particles to wood, and thus the adhesives are required to be nearly colorless, to minimize the effect on the original color of the pigments. Water-based pigments are commonly mixed with animal glues, such as fish glue and bone glue [15]. Oil-based pigments were found to be mixed with castor oil, linseed oil, and tung oil [16], and emulsion pigments are mixed with eggs and egg whites [17]. It has been reported that the adhesives can be used alone or mixed with others. For instance, the use of both egg white and animal glue was found in the painting of Longju Temple in Sichuan [18]. Some pigments on the painting have been nearly peeling off, probably due to degradation of the adhesives. In this study, we used pyrolysis-gas chromatography/mass spectrometry (Py-GC/MS) to detect ageing products and identify the compositions of the adhesives, such as animal glue, egg yolk and glass glue, tung oil and casein [19], etc.

In recent decades, most of the literature has focused on paintings on murals and clay sculptures, while the color paintings on ancient wooden architecture, e.g., at the Taiping Heavenly Kingdom Prince Dai's mansion, whose painting process is rarely applied in other countries except Asia, has not been fully studied or reported before. Small amounts of samples were taken from the painting in this study, and the composition of the pigments and adhesives used in the samples were analyzed.

**Table 1.** Summary of identified pigments for paintings on ancient wooden buildings, sampling points, techniques used for pigment identification, and corresponding literature.

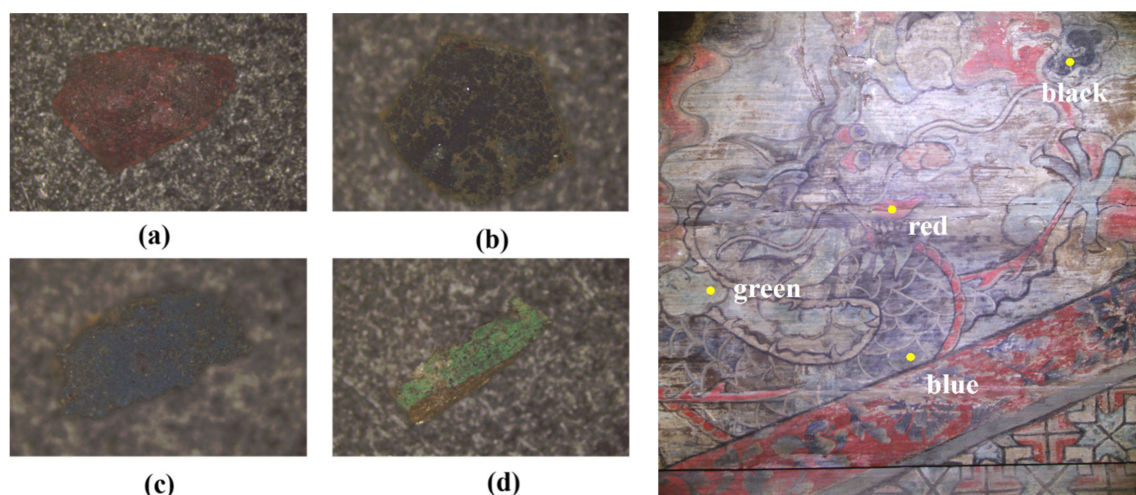
Color	Date (Century)	Pigments	Sample	Techniques	Literature	
Red	9th	Cinnabar (HgS)	Foguang Temple Hall	SEM-EDX, Raman, FI-IR	Fu et al. (2015) [20]	
	15th		Longju Temple	SEM-EDS, Raman	Chen et al. (2019) [18]	
	16th		Dagaoxuan Temple	SEM-EDS, Raman, PLM	Lei et al. (2017) [21]	
	16th		Yanxi Hall	SEM-EDS, Raman	Liu et al. (2018) [22]	
	9th	Red lead (Pb <sub>3</sub> O <sub>4</sub> )	Foguang Temple Hall	SEM-EDX, Raman, FI-IR	Fu et al. (2015) [20]	
	18th		Altar of Agriculture	Raman, ED-XRF	Li et al. (2021) [23]	
	16th	Hematite ( $\alpha$ -Fe <sub>2</sub> O <sub>3</sub> )	Dagaoxuan Temple	SEM-EDS, Raman, PLM	Lei et al. (2017) [21]	
	16th		Yanxi Hall	SEM-EDS, Raman	Liu et al. (2018) [22]	
Green	15th	Emerald [Cu(CH <sub>3</sub> COO) <sub>2</sub> ·3Cu(AsO <sub>2</sub> ) <sub>2</sub> ]	building in the Jiangxue Palace	EDX, Raman, PLM	Fu et al. (2020) [24]	
	15th		Wuying Hall of the Imperial Palace	EDX, m-RS	Shen et al. (2006) [25]	
	16th		Dagaoxuan Temple	SEM-EDS, Raman, PLM	Lei et al. (2017) [21]	
	19th		Summer Palace	SEM-EDS, XRD	Ma et al. (2019) [26]	
	9th		Atacamite [Cu <sub>2</sub> (OH) <sub>3</sub> Cl]	Foguang Temple Hall	SEM-EDX, Raman, FI-IR	Fu et al. (2015) [20]
	15th			Longju Temple	SEM-EDS, Raman	Chen et al. (2019) [18]
	16th			Yanxi Hall	SEM-EDS, Raman	Liu et al. (2018) [22]
	18th			Altar of Agriculture	Raman, ED-XRF	Li et al. (2021) [23]

Table 1. Cont.

Color	Date (Century)	Pigments	Sample	Techniques	Literature	
White	15th	Lead white [2PbCO <sub>3</sub> ·Pb(OH) <sub>2</sub> ]	building in the Jiangxue Palace	SEM-EDS, Raman, PLM	Fu et al. (2020) [24]	
	18th		Altar of Agriculture	Raman, ED-XRF	Li et al. (2021) [23]	
	15th	Chalk (CaCO <sub>3</sub> )	Wuying Hall of the Imperial Palace	EDX, m-RS	Shen et al. (2006) [25]	
	16th	Hydrocerussite [2PbCO <sub>3</sub> ·Pb(OH) <sub>2</sub> ·H <sub>2</sub> O]	Dagaoxuan Temple	SEM-EDS, Raman, PLM	Lei et al. (2017) [21]	
	16th	Gypsum (CaSO <sub>4</sub> )	Dagaoxuan Temple	SEM-EDS, Raman, PLM	Lei et al. (2017) [21]	
	9th	Kaolinite [Al <sub>2</sub> Si <sub>2</sub> O <sub>5</sub> (OH) <sub>4</sub> ]	Foguang Temple Hall	SEM-EDX, Raman, FI-IR	Fu et al. (2015) [20]	
Blue	15th	Ultramarine [(Na,Ca) <sub>8</sub> (AlSiO <sub>4</sub> ) <sub>6</sub> (S <sub>2</sub> Cl) <sub>2</sub> ]	Wuying Hall of the Imperial Palace	EDX, m-RS	Shen et al. (2006) [25]	
	16th		Dagaoxuan Temple	SEM-EDS, Raman, PLM	Lei et al. (2017) [21]	
	16th		Yanxi Hall	SEM-EDS, Raman	Liu et al. (2018) [22]	
	19th		Summer Palace	SEM-EDS, EDS, XRD	Ma et al. (2019) [26]	
	9th		Azurite [2CuCO <sub>3</sub> ·Cu(OH) <sub>3</sub> ]	Foguang Temple Hall	SEM-EDX, Raman, FI-IR	Fu et al. (2015) [20]
	15th			Longju Temple	SEM-EDS, Raman	Chen et al. (2019) [18]
	16th			Yanxi Hall	SEM-EDS, Raman	Liu et al. (2018) [22]
	18th			Altar of Agriculture	Raman, ED-XRF	Li et al. (2021) [23]
18th	Indigo [C <sub>16</sub> H <sub>10</sub> N <sub>2</sub> O <sub>2</sub> ]	Temple of Confucius	Raman	Li (2015) [27]		
Black	15th	Graphite (C)	Wuying Hall of the Imperial Palace	EDX, m-RS	Shen et al. (2006) [25]	
	15th		Longju temple	SEM-EDS, Raman	Chen et al. (2019) [18]	
	16th		Dagaoxuan Temple	SEM-EDS, Raman, PLM	Lei et al. (2017) [21]	
	18th		Altar of Agriculture	Raman, ED-XRF	Li et al. (2021) [23]	
Yellow	18th	Litharge (γ-PbO)	Altar of Agriculture	Raman, ED-XRF	Li et al. (2021) [23]	
	16th	Chrome (PbCrO <sub>4</sub> )	Dagaoxuan Temple	SEM-EDS, Raman, PLM	Lei et al. (2017) [21]	
	18th		Altar of Agriculture	Raman, ED-XRF	Li et al. (2021) [23]	
	16th	Realgar (As <sub>4</sub> S <sub>4</sub> )	Dagaoxuan Temple	SEM-EDS, Raman, PLM	Lei et al. (2017) [21]	
	16th	Orpiment (As <sub>2</sub> S <sub>3</sub> )	Dagaoxuan Temple	SEM-EDS, Raman, PLM	Lei et al. (2017) [21]	

## 2. Materials

Samples were collected from the flaking pigments on the color painting on the northern beam of the main hall in the mansion. In order to keep the painting as intact as possible, small amounts of samples were taken from four areas (Figure 2). The pigment particles were firstly observed using a polarized-light microscope, then elemental analysis was carried out using SEM-EDS, and pigment compositions and structures were finally identified using m-RS and FTIR spectrometers. The organic adhesive in the pigment samples was characterized using Py-GC/MS.



**Figure 2.** Four pigment samples (left) collected from the color painting (right) on the northern beam of the main hall in the mansion (a) red, (b) black, (c) blue, and (d) green pigment), as labeled with yellow dots.

### 3. Experimental Methods and Instrumentation

#### 3.1. Energy Dispersive Spectrometry (EDS)

Elemental analyses were conducted using a scanning electron microscope equipped with an energy-dispersive X-ray spectrometer (SEM-EDS, HITACHI SU3500, Japan) with a high performance silicon drift detector and X-ray tube (Rh target); the test range was 11NA–92U. The corresponding results are shown in Table 2.

**Table 2.** A summary of techniques used for pigment analyses and elemental compositions for corresponding pigment samples.

Sample	Color	Experimental Methods	Elements
1	Red	EDS, m-RS, PLM, Py-GC/MS	Hg (50.20%), N (32.8%), P (10.24%), Ca (3.09%), C (1.98%)
2	Black	EDS, m-RS, PLM	C (65.56%), P (14.16%), Fe (9.57%), Ca (9.23%), K (1.98%)
3	Blue	EDS, m-RS, PLM, FT-IR	N (35.47%), O (27.42%), Ca (27.29%), C (9.3%), Si (0.5%)
4	Green	EDS, m-RS, PLM, FT-IR	N (55.13%), Cl (17.19%), P (12.09%), Ca (5.91%), Cu (4.91%)

#### 3.2. Micro-Raman Spectroscopy (m-RS)

Raman spectra were recorded using a LabRAM HR Evolution Raman Microscope (inVia Qontor Renishaw, UK) with an 1800 grooves/mm grating and a coupled m-RS charge detector. The excitation wavelengths were 532 nm and 785 nm. A 50× objective lens was used to observe the pigments, and the acquisition range was from 100 to 2000 wavenumbers ( $\text{cm}^{-1}$ ). Spectra of red, black, and green pigments were obtained using 532 nm, and the Raman spectrum for the blue pigment was collected using 785 nm.

#### 3.3. Polarized Light Microscopy (PLM)

Polarized light microscopy (Olympus BX53M, Shinjuku, Japan) was used to observe pigment morphology under 5–100× objectives, before which the samples were pre-processed. The pigment samples were soaked in ethanol for 30 min and then placed onto the microscope slide. After ethanol evaporation, the cover glass was placed over the samples, and then the heated and melted resin was dropped through the gap between the slide and cover glass to immobilize the sample particle.

### 3.4. Fourier-Transform Infrared Spectroscopy (FT-IR)

KBr was placed in an oven at 180 °C and dried for 24 h; 150 mg of dried KBr was ground as a blank sample and mixed with 2 mg of ground pigment samples. The sample powders were pressed and then scanned using the FTIR spectroscope (Thermo Scientific Nicolet iS10, Waltham, MA, USA) for detection in the wavelength range of 450–4000  $\text{cm}^{-1}$  with the spectral resolution at 1  $\text{cm}^{-1}$ .

### 3.5. Pyrolysis-Gas Chromatography/Mass Spectrometry (Py-GC/MS)

About 50  $\mu\text{g}$  of pigment sample was placed into a thermal pyrolyzer, with 3  $\mu\text{L}$  of 20% *w/w* tetramethylammonium hydroxide (TMAH) added for pre-treatment. The sample was then placed in an autosampler and pyrolyzed at 600 °C after resting for 1 h. After the pyrolysis, the generated products were identified by using GC-MS.

The Py-GC/MS consists of two parts. Parameters of the first part for pyrolysis (Frontier Labs EGA/PY-3030D Koriyama, Japan) include thermal cracking temperature, thermal cracking time, syringe temperature, and interface temperature of the syringe and chromatograph, which were set at 600 °C, 10 s, 250 °C, and 320 °C, respectively. The other part includes GC/MS (Shimadzu QP2010 Ultra, Kyoto, Japan) and a SLB-5MS chromatography column (5% diphenyl-95% dimethylsiloxane). The initial temperature of the oven containing the column was set to 50 °C, and this was held for 5 min. The temperature was then increased at a rate of 3 °C/min to a final temperature of 292 °C that was held for 3 min. The pre-column pressure, the flow rate, and the separation ratio were set at 15.4 kPa, 0.6 mL/min, and 1:100, respectively, and the ionization voltage, scan rate, and mass-to-charge ratio of the mass spectrometer were set at 70 eV, 0.5 s, and 50 to 750, respectively.

## 4. Results and Discussion

### 4.1. Pigments

#### 4.1.1. Red

PLM was used to examine the red pigment samples, showing dark reddish color under horizontal polarized light (Figure 3a) or reddish orange under perpendicular polarized light (Figure 3b), suggesting that cinnabar might be present. This was further explored using other techniques. The Raman spectrum of the red pigment sample shows peaks at 254  $\text{cm}^{-1}$  (vs), 285  $\text{cm}^{-1}$  (w), and 349  $\text{cm}^{-1}$  (w) (Figure 4). Comparing the Raman spectrum of the red sample with the standard spectrum, the peak at 254  $\text{cm}^{-1}$  is attributed to the stretching vibrational band of Hg-S and the bands at 285  $\text{cm}^{-1}$  (w) and 349  $\text{cm}^{-1}$  (w) belong to the degenerate E modes, which can be assigned to the normal modes  $E_{LO}$  and  $E_{TO}$  [28], confirming the presence of cinnabar, which is consistent with the EDS results (Table 2). The lack of interference from the fluorescent background of the Raman spectrum indicates the high purity of the red pigment.

Cinnabar, the most widely used red pigment, is commonly used alone in a number of Chinese paintings in tombs and clay sculptures, e.g., at Xialu Temple [29], The Temple of Venus [30], a Roman temple [31], the polychrome arhat at the Lingyan Temple [32], the Song Dynasty Polychrome Statue-Making of Sage Mother Hall of the Jinci Temple [33], and a polychrome clay sculpture of Hua Yan Temple of the Liao Dynasty [11]. Due to its toxicity, it is able to control the growth of most of pests and mold. The discovery and use of mercury ore in China can be dated back to 6000 years ago [34], and objects containing cinnabar have been found in the Hemudu Site (5000–3300 BC) and the Longshan Site (2500–2000 BC). Excavations at the Yinxu site, built during Shang dynasty, revealed that cinnabar was used to paint Shang oracle bones [35], and in the Song dynasty a small amount of cinnabar was used in the production of medicine [36].

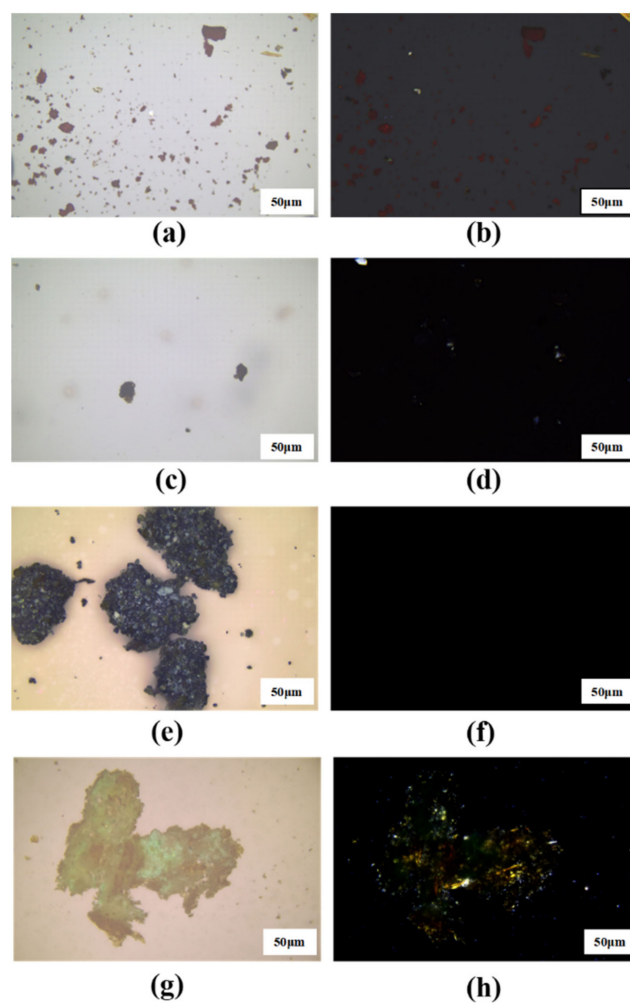


**Figure 3.** PLM images observed under horizontal and perpendicular polarized light for (a,b) red, (c,d) black, (e,f) blue, and (g,h) green pigments. All samples were observed under 20× magnifications. The sampling positions are shown in Figure 2.

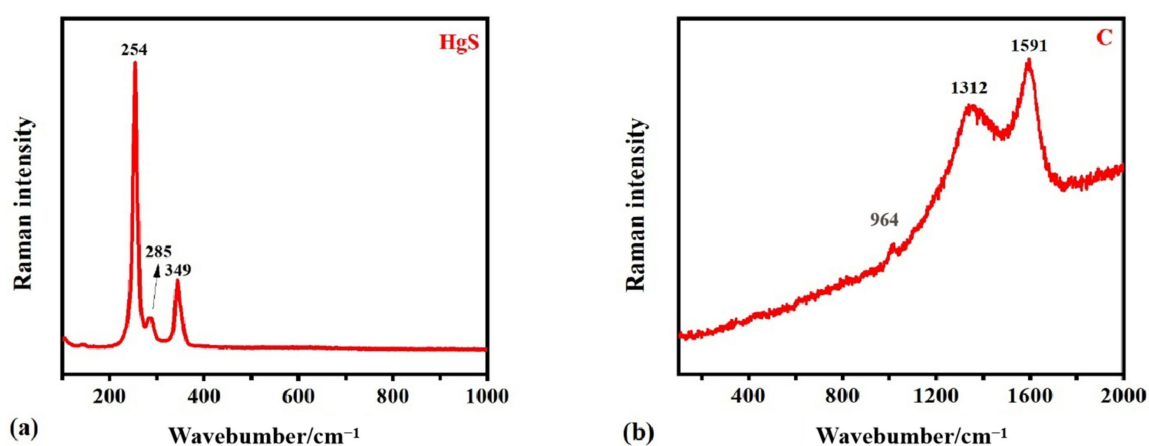


**Figure 4.** Raman spectrum of the (a) red and (b) black pigment samples.

#### 4.1.2. Black

A few types of black pigments are available for paintings, such as carbon black or ivory black (C), iron black ( $\text{Fe}_3\text{O}_4$ ), lead dioxide ( $\text{PbO}_2$ ), etc. Black pigment has long been used in historic colored paintings, as summarized in Table 1. EDS analysis results (Table 2) show that carbon occupies the highest proportion of the black pigment sample at 65.56%,

so it is highly possible that the pigment is mainly composed of carbon black or ivory black. However, the presence of Ca (9.23%) and P (14.16%) indicate that the black pigment might be ivory black, whose composition includes calcium phosphate, calcium carbonate, and carbon. This was then further confirmed by determining the composition of the sample using a Raman spectroscope (Figure 4). The standard Raman spectrum of ivory black shows bands at  $964\text{ cm}^{-1}$ ,  $1316\text{ cm}^{-1}$ , and  $1593\text{ cm}^{-1}$  [37] for our black pigment sample (Figure 4b); the peak at  $964\text{ cm}^{-1}$  can be attributed to the biomineral apatite  $[\text{Ca}_3(\text{PO}_4)_2]$  [38], the peak at  $1591\text{ cm}^{-1}$  was attributed to the G-band (C=C) [39], while the coordination state at  $1312\text{ cm}^{-1}$  is still controversial. Currently, the most accepted concept is that this peak belongs to C-C bonds with  $\text{sp}^3$  hybridization (mode  $\text{A}_{1g}$ ) in diamond [40]. Additionally, using PLM, under the horizontal polarized light (Figure 3c), the black pigment sample is irregular and has no visible edge, and under perpendicular polarized light (Figure 3d), no imaging is present, verifying the presence of ivory black. Ivory black is a fine black pigment made by calcining ivory. Due to protection of elephants, the raw materials have been gradually substituted by animal bones, e.g., carbonized cow or sheep bones [41].

#### 4.1.3. Blue

Given that element analysis for the blue pigment shows the presence of N, O, Ca, C, and Si (Table 2), it was initially speculated that the blue pigment might be smalt (potassium glass containing cobalt: 65%  $\text{SiO}_2$ , 16%–21%  $\text{K}_2\text{O}$ , and 6%–7%  $\text{CoO}$  with impurities Ba, Ca, and Fe), ultramarine  $[(\text{Na,Ca})_8(\text{AlSiO}_4)_6(\text{SCl})_2]$ , or indigo ( $\text{C}_{16}\text{H}_{10}\text{N}_2\text{O}_2$ ). The detected Ca (27.29%) and Si (0.5%) might be from impurities such as dust deposition on the painting surface. Additionally, the origin of Ca might be from the addition of calcium carbonate to the pigment, which is a common technology that increases the coverage rate. In order to further investigate the composition of the blue pigment sample, the Raman spectrum and FT-IR spectrum were collected, as shown in Figure 5a,b.

The peaks at  $1339\text{ cm}^{-1}$  (m) and  $1539\text{ cm}^{-1}$  (vs) in the Raman spectrum demonstrate that the blue pigment sample might be indigo, as the spectrum is consistent with the standard and the Raman spectra of the other blue pigments do not show characteristic bands at the two positions, in which the peak at  $1339\text{ cm}^{-1}$  (m) is an in-plane curved N-H stretching band and  $1539\text{ cm}^{-1}$  (vs) is attributed to symmetric C=C stretching [42]. In addition, the FT-IR spectrum in Figure 5b further confirms the presence of indigo, where the bands at  $3430\text{ cm}^{-1}$ ,  $1626\text{ cm}^{-1}$ , and at both  $1462\text{ cm}^{-1}$  and  $1319\text{ cm}^{-1}$  belong to asymmetric stretching of N-H, the C=O stretching band, and stretching vibrations of C-C as well as in-plane deformation of C-H, respectively [43]. It can be seen from the PLM images that the blue pigment changes from light bluish to dark bluish under horizontal polarized light (Figure 3e) and is fully extinguished under perpendicular polarized light (Figure 3f).

Indigo is an organic pigment extracted from plants throughout a complicated production process and is relatively stable among organic pigments [44]. In 1880, the German scientist Bayer achieved synthesis of this dye, leading to indigo production beginning to be industrialized in 1897. The use of indigo can be traced back to 6000 years ago by the discovery of several textile fragments at the site of Huaca Prieta, Peru, in 2009 [45]. Indigo was rarely applied in most of ancient Chinese architectural paintings, where mineral pigments such as azurite and ultramarine were more frequently used [25]. It is commonly found in excavated silk weavings in China, e.g., indigo-dyed silks were excavated from the Mawangdui Han tomb of the Western Han Dynasty, from about 2200 years ago [46], and is found on other types of objects in other countries, e.g., funerary objects from the Chupicuaro culture [47] and the pre-classic and classic monumental architecture of the ancient pre-Columbian city of Calakmul [48].

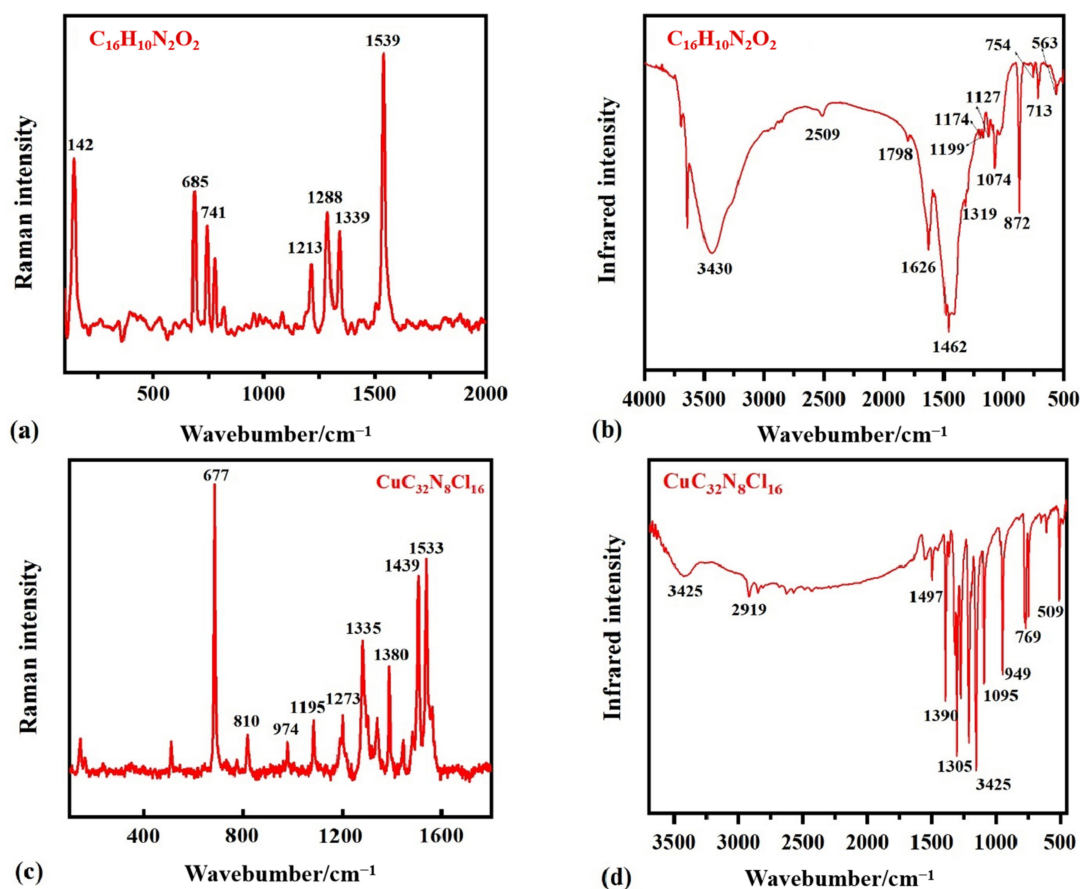


**Figure 5.** (a) Raman spectrum and (b) FT-IR spectrum for the blue pigment sample (indigo,  $C_{16}H_{10}N_2O_2$ ); (c) Raman spectrum and (d) FT-IR spectrum for the green pigment (phthalocyanine green,  $CuC_{32}N_8Cl_{16}$ ).

#### 4.1.4. Green

Using PLM, under horizontal polarized light (Figure 3g), the green pigment particles gathering in clusters are bright and fine, without the characteristics of typical mineral pigments, and the particles show light extinction under the perpendicular polarized light (Figure 3h). These properties indicate that the green pigment might be organic. As shown in Table 2, the green pigment sample contains N, Cl, P, Ca, and Cu, in which Cu is the characteristic element and Ca is rarely present in the green pigment. It is assumed that the Ca was also probably from impurities such as dust deposition and that the green pigment might be malachite [ $CuCO_3 \cdot Cu(OH)_2$ ], atacamite [ $Cu_2(OH)_3Cl$ ], Paris green [ $Cu(CH_3COO)_2 \cdot 3Cu(AsO_2)_2$ ], or phthalocyanine green ( $CuC_{32}N_8Cl_{16}$ ).

The Raman spectrum demonstrates that the peaks at  $677\text{ cm}^{-1}$  (s),  $1439\text{ cm}^{-1}$  (s), and  $1533\text{ cm}^{-1}$  (s) in Figure 5c are consistent with the standard spectrum of phthalocyanine green ( $CuC_{32}N_8Cl_{16}$ ). In addition, this pigment shows a unique FT-IR spectrum (Figure 5d) where the band at  $2919\text{ cm}^{-1}$  belongs to the C-H asymmetric stretching vibrations, quite a few sharp peaks [49] in band range of  $1700\text{--}500\text{ cm}^{-1}$  are attributed to the stretching deformation of the C-C in the aromatic ring system and the in-plane and out-of-plane bending of the C-H bond of the ring system, and the peak at  $949\text{ cm}^{-1}$  belongs to out-of-plane bending modes of N-Cu and C-Cl [50].

Phthalocyanine green is a synthetic organic pigment which has good stability under UV light and high temperature. Given that phthalocyanine green was found in 1936 [51] and the local government did not give attention to the mansion until 1976 [52], this indicates that the painting was probably repaired or refurbished in mid-20th century (1936–1976). The use of this pigment in paintings of ancient Chinese buildings is rarely recorded, and, to

our knowledge, phthalocyanine green was only used in conservation of the paintings in Longju Temple in Sichuan [18] and in early 20th century Russian painting [53].

#### 4.2. Adhesive

It is difficult to directly execute mineral and organic pigment particles on color paintings; therefore, adhesives are used. In this study, the red pigment sample was analyzed using Py-GC/MS to identify the adhesive, the total ion chromatogram of the sample was obtained (Table 3 and Figure 6), and the corresponding pyrolysis by-products are shown in Table 3. Due to the application of the methylation technique, most of generated products were determined to be methylation-related. The results demonstrate that many products were pyrolyzed from proteins [54,55], such as 1H-Pyrrole, 1-methyl- (peak 5), pyridine (peak 6), valine (peak 10), alanine (peak 12), glycine (glue, egg white) (peak 14), and methyl ester (peak 7/21/23/25/26) [56]. Over long-time natural aging, contents of these products are decreased compared with that of the fresh glue. The peaks at No. 13 and 15 indicate the presence of glue marker (fish glue) and protein, suggesting the use of glue mainly containing protein [15]. Over long-time aging, the contents of protein decreased compared with that of the fresh glue, indicating the glue degradation on the flaking area of the painting. As many studies suggest [16], the adhesive used for different pigments are often the same on the same painting; we therefore carried out adhesive identification for the red pigment sample only in this study.

**Table 3.** Component compositions of the red pigment sample.

Peak Number	Retention Time (min)	Area (%)	Compound
1	1.5363	0.18	Furan, 3-methyl-
2	1.8173	26.97	Methylamine, N, N-dimethyl
3	2.1037	0.30	Benzene
4	2.816	0.77	Acetic acid
5	3.3073	0.48	1H-Pyrrole, 1-methyl-
6	3.5067	0.45	Pyridine
7	3.543	0.13	Propanoic acid, 2-methoxy-, methyl ester
8	4.717	2.56	Cyclotrisiloxane, hexamethyl
9	5.5797	0.07	Dimethyl sulfate
10	7.8797	0.01	Valine
11	8.495	0.14	3-Methylanisole
12	9.9147	0.25	Alanine
13	10.237	0.18	Glue marker (fish glue 108/139)
14	10.755	0.02	glycine (glue, egg white)
15	11.7573	0.17	Protein
16	12.113	0.05	phenol formaldehyde resin (TMAH)
17	14.1283	6.27	Schellmannose
18	14.8763	0.19	1,2,3,4-Tetramethoxybenzene
19	15.0867	0.05	Diarylide, RI = 2338
20	15.3487	0.85	Benzaldehyde, 3,4-dimethoxy
21	16.823	0.12	orsellinic acid, 2,4-di-O-methyl, methyl ester
22	20.0143	1.28	hexadecenoic acid, methyl ester. FA-C16:1
23	20.2363	3.59	Hexadecanoic acid, methyl ester
24	21.7787	0.59	Benzene, 1,1'-(1-methylethylidene) bis [4-methoxy-]
25	21.9367	0.90	9-Octadecenoic acid (Z)-, methyl ester
26	22.16	1.74	Octadecanoic acid, methyl ester

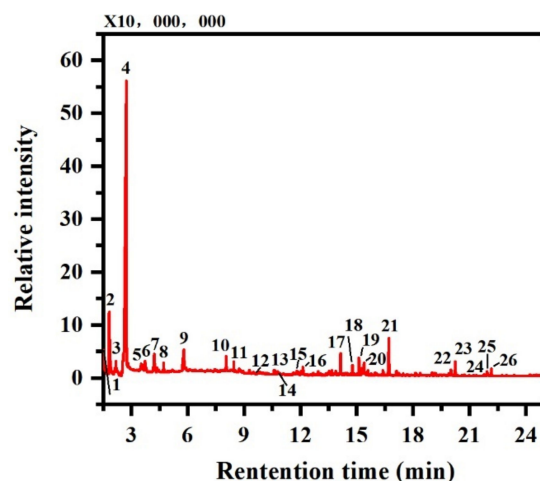


Figure 6. The total ion chromatogram (TIC) of the red pigment samples.

The contents of fatty acids were also detected by Py-GC/MS for the red pigment sample (Figure 7), including monocarboxylic and dicarboxylic fatty acids, both of which are typical pyrolysis products of dry oil [57]. The ratio of palmitic acid to stearic acid (P/S) is often used to differentiate various types of dry oils, i.e., P/S values are 0.9–1.1 for boiled tung oil, 1.3–1.6 for raw tung oil, 1.2–1.5 for linseed oil, 1.6–1.8 for poppy oil, and 1.8–2.0 for walnut oil [58]. The determined P/S value of the dry oil in our sample is at 1.96, indicating that the red pigment sample might contain walnut oil. This assumption is further verified by the presence of methylamine and N, N-dimethyl- (peak 2) in the obtained pyrolysis products (Table 3) [59]. The use of the walnut oil might be related to the craftsmanship of the color paintings on the wooden architecture, where oil is applied in wood surface for better painting before executing pigments. As reported in many studies [60], tung oil is the most widely used, indicating that the use of the walnut oil is a unique painting process for paintings in the mansion for Price Dai.

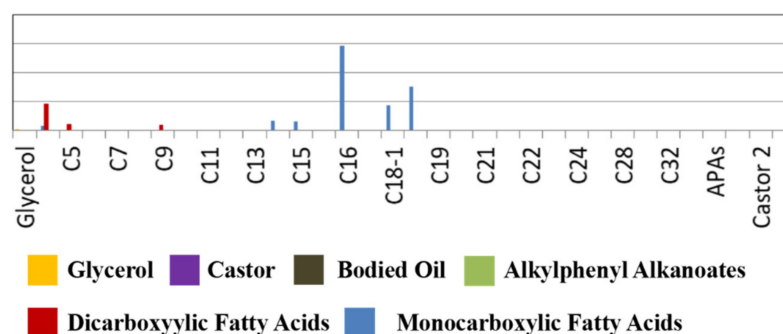


Figure 7. The relative concentrations of fatty acids for the red pigment sample obtained by Py-GC/MS; carboxylic acid with carbon numbers of n.

## 5. Conclusions

In this study, a comprehensive analysis was performed for four pigment samples collected from a flaking area on a color painting on ancient wooden architecture in the Taiping Heavenly Kingdom Prince Dai's mansion. A series of techniques were used, mainly including EDS, PLM, m-RS, and FT-IR.

The results show that the red and black pigments, identified to be cinnabar (Hg-S) and ivory black (C), respectively, are consistent with the most-used traditional Chinese pigments as applied in a variety of heritage objects. In addition, interestingly, the blue and green pigments were determined to be organic, specifically indigo ( $C_{16}H_{10}N_2O_2$ ) and phthalocyanine green ( $CuC_{32}N_8Cl_{16}$ ) respectively. However, indigo is hardly used in most traditional Chinese architectural paintings, which is one of the unique features of these

painting materials. Since phthalocyanine green was invented in 1936, it is inferred that the green pigment was repainted later; we therefore speculate that this ancient wooden architecture has been refurbished. It is worth noting that this green pigment was rarely used in traditional Chinese color painting on ancient wooden architecture.

Using Py-Gc/Ms analysis, the presence of protein demonstrates that glue mainly containing protein was used as adhesive for adhering pigment particles. Over long-time natural aging, the contents of protein decreased, indicating glue degradation on the flaking area of the painting. It is found that walnut oil was used on the wood before painting as a primer, which is different from the traditionally used oil, i.e., tung oil.

This study has expanded our understanding of the main pigments and adhesive used for the color painting in the Taiping Heavenly Kingdom Prince Dai's mansion, in which several uncommon painting materials were applied, giving data support and evidence for future conservation and better management. More research is needed to comprehensively evaluate the condition of other paintings in the mansion for better preventive and intervention conservation treatment, such as prevention of the deterioration caused by microorganisms, which will be one of our future works.

**Author Contributions:** Conceptualization, K.H. and Y.L. (Yuhu Li); resources, H.Y.; methodology, G.T.; investigation, S.H.; software, J.L.; formal analysis, Y.L. (Yanli Li); data curation, E.M.; writing—original draft preparation, Y.L. (Yujia Luo) and Y.T.; visualization, P.F.; writing—review and editing, Y.L. (Yujia Luo); supervision, project administration and funding acquisition, Y.L. (Yuhu Li). All authors have read and agreed to the published version of the manuscript.

**Funding:** This work was supported by the National Cultural Heritage Administration of China, Mercedes Benz and Beijing Foundation for the Protection of Cultural Relics of the Forbidden City [Study on Conservation Effect Evaluation of Ancient Architecture Painting Technology].

**Acknowledgments:** This work was supported by the project of the Jinhua Cultural Heritage Administration of Taiping Heavenly Kingdom Prince Dai's mansion in Jiangsu, China.

**Conflicts of Interest:** The authors declare no conflict of interest.

## References

1. Zhou, W.; Wang, L. Production techniques of paintings and colored drawings of ancient architecture. *Sci. Conserv. Archaeol.* **2010**, *22*, 1–9.
2. Guo, L. A Brief Analysis of the Decorative Art Features of Lacquered Coffin Painting in Mawangdui. Master's Thesis, Nanjing University of the Arts, Nanjing, China, 2010.
3. Liu, J.-H.; Ke, W.; Hwang, M.-C.; Chen, K.Y. Micro-Raman spectroscopy of Shang oracle bone inscriptions. *J. Archaeol. Sci. Rep.* **2021**, *37*, 102910. [[CrossRef](#)]
4. Mahmoud, H.H.M.; El-Badry, A. Physicochemical characterization of building and painting materials from the Ptolemaic Osirian catacombs of Karnak temples, Upper Egypt. *Eur. Phys. J. Plus* **2020**, *135*, 741. [[CrossRef](#)]
5. Kawahito, M.; Urakawa, H.; Ueda, M.; Kajiwara, K. Color in cloth dyed with natural indigo and synthetic indigo. *Sen. I Gakkaishi* **2002**, *58*, 122–128. [[CrossRef](#)]
6. Abel, A. The history of dyes and pigments: From natural dyes to high performance pigments. In *Colour Design: Theories and Applications*, 2nd ed.; Woodhead Publishing Limited: Cambridge, UK, 2017.
7. Richhariya, G.; Kumar, A. Fabrication and characterization of mixed dye: Natural and synthetic organic dye. *Opt. Mater.* **2018**, *79*, 296–301. [[CrossRef](#)]
8. Fu, P.; Teri, G.-L.; Li, J.; Li, J.-X.; Li, Y.-H.; Yang, H. Investigation of ancient architectural painting from the Taidong Tomb in the Western Qing tombs, Hebei, China. *Coatings* **2020**, *10*, 688. [[CrossRef](#)]
9. Go, I.; Mun, S.; Lee, J.; Jeong, H. A case study on Hoeamsa Temple, Korea: Technical examination and identification of pigments and paper unearthed from the temple site. *Herit. Sci.* **2022**, *10*, 20. [[CrossRef](#)]
10. Klisinska-Kopacz, A. Non-destructive characterization of 17th century painted silk banner by the combined use of Raman and XRF portable systems. *J. Raman Spectrosc.* **2015**, *46*, 317–321. [[CrossRef](#)]
11. Wang, X.; Zhen, G.; Hao, X.Y.; Tong, T.; Ni, F.F.; Wang, Z.; Jia, J.; Li, L.; Tong, H. Spectroscopic investigation and comprehensive analysis of the polychrome clay sculpture of Hua Yan Temple of the Liao Dynasty. *Spectrochim. Acta Part A Mol. Biomol. Spectrosc.* **2020**, *240*, 118574. [[CrossRef](#)]
12. Gard, F.S.; Santos, D.M.; Daizo, M.B.; Freire, E.; Reinoso, M.; Halac, E.B. Pigments analysis of an Egyptian cartonnage by means of XPS and Raman spectroscopy. *Appl. Phys. A Mater. Sci. Process.* **2020**, *126*, 218. [[CrossRef](#)]

13. Cerrato, E.J.; Cosano, D.; Esquivel, D.; Otero, R.; Jiménez-Sanchidrián, C.; Ruiz, J.R. A multi-analytical study of a wall painting in the Satyr domus in Córdoba, Spain. *Spectrochim. Acta Part A Mol. Biomol. Spectrosc.* **2020**, *232*, 118148. [[CrossRef](#)] [[PubMed](#)]
14. Dawson, P. The vibrational spectrum of  $\alpha$ -mercuric sulphide. *Spectrochim. Acta Part A Mol. Spectrosc.* **1972**, *28*, 2305–2310. [[CrossRef](#)]
15. Wang, X.; Zhen, G.; Hao, X.; Zhou, P.; Wang, Z.; Jia, J.; Gao, Y.; Dong, S.; Tong, H. Micro-Raman, XRD and THM-Py-GC/MS analysis to characterize the materials used in the Eleven-Faced Guanyin of the Du Le Temple of the Liao Dynasty, China. *Microchem. J.* **2021**, *171*, 106828. [[CrossRef](#)]
16. Kurouski, D.; Zaleski, S.; Casadio, F.; Van Duyne, R.P.; Shah, N.C. Tip-enhanced Raman spectroscopy (TERS) for in situ identification of indigo and iron gall ink on paper. *J. Am. Chem. Soc.* **2014**, *136*, 8677–8684. [[CrossRef](#)] [[PubMed](#)]
17. Orsini, S.; Parlanti, F.; Bonaduce, I. Analytical pyrolysis of proteins in samples from artistic and archaeological objects. *J. Anal. Appl. Pyrolysis* **2017**, *124*, 643–657. [[CrossRef](#)]
18. Chen, E.; Zhang, B.; Zhao, F.; Wang, C. Pigments and binding media of polychrome relics from the central hall of Longju temple in Sichuan, China. *Herit. Sci.* **2019**, *7*, 45. [[CrossRef](#)]
19. Hao, X.; Schilling, M.R.; Wang, X.; Khanjian, H.; Heginbotham, A.; Han, J.; Auffret, S.; Wu, X.; Fang, B.; Tong, H. Use of THM-PY-GC/MS technique to characterize complex, multilayered Chinese lacquer. *J. Anal. Appl. Pyrolysis* **2019**, *140*, 339–348. [[CrossRef](#)]
20. Fu, J.; Bai, X.; Huang, F. Study on making materials and technology of color painting in East Hall of Foguang Temple. *J. Chin. Antiq.* **2015**, *129*, 73–77.
21. Lei, Z.; Wu, W.; Shang, G.; Wu, Y.; Wang, J. Study on colored pattern pigments of a royal Taoist temple beside the Forbidden City (Beijing, China). *Vib. Spectrosc.* **2017**, *92*, 234–244. [[CrossRef](#)]
22. Liu, L.; Zhang, B.; Yang, H. The Analysis of the colored paintings from the Tanxi Hall in the Forbidden City. *Spectrosc. Spectr. Anal.* **2018**, *38*, 68–77.
23. Li, Y.; Wang, F.P.; Ma, J.J.; He, K.; Zhang, M. Study on the pigments of Chinese architectural colored drawings in the Altar of Agriculture (Beijing, China) by portable Raman spectroscopy and ED-XRF spectrometers. *Vib. Spectrosc.* **2021**, *116*, 103291. [[CrossRef](#)]
24. Fu, P.; Teri, G.; Li, J.; Huo, Y.; Yang, H.; Li, Y. Analysis of an ancient architectural painting from the Jiangxue palace in the imperial museum, Beijing, China. *Anal. Lett.* **2021**, *54*, 684–697. [[CrossRef](#)]
25. Shen, A.G.; Wang, X.H.; Xie, W.; Shen, J.; Li, H.Y.; Liu, Z.A.; Hu, J.M. Pigment identification of colored drawings from Wuying Hall of the Imperial Palace by micro-Raman spectroscopy and energy dispersive X-ray spectroscopy. *J. Raman Spectrosc.* **2006**, *37*, 230–234. [[CrossRef](#)]
26. Ma, Z.; Wang, L.; Yan, J.; Zhou, W.; Pitthard, V.; Bayerova, T.; Krist, G. Chromatographic, microscopic, and spectroscopic characterization of a wooden architectural painting from the Summer Palace, Beijing, China. *Anal. Lett.* **2019**, *52*, 1670–1680. [[CrossRef](#)]
27. Jing, L. The Composition of pigments of decorative paintings on ancient building of Qufu's Temple of Confucius. *China Cult. Herit. Sci. Res.* **2014**, *4*, 86–89.
28. Cosano, D.; Esquivel, D.; Costa, C.M.; Jimenez-Sanchidrian, C.; Ruiz, J.R. Identification of pigments in the Annunciation sculptural group (Cordoba, Spain) by micro-Raman spectroscopy. *Spectrochim. Acta Part A Mol. Biomol. Spectrosc.* **2019**, *214*, 139–145. [[CrossRef](#)]
29. Lei, Y.; Wang, S. Material analysis of the wall paintings in Xialu Temple, Tibet Autonomous Region, China. *Stud. Conserv.* **2014**, *59*, 314–327. [[CrossRef](#)]
30. Piovesan, R.; Siddall, R.; Mazzoli, C.; Nodari, L. The Temple of Venus (Pompeii): A study of the pigments and painting techniques. *J. Archaeol. Sci.* **2011**, *38*, 2633–2643. [[CrossRef](#)]
31. Mahmoud, H.M.; Hussein, M.; Brania, A. Pigments and plasters from the Roman temple of Deir El-Hagar, Dakhla Oasis, Egypt: Vibrational spectroscopic characterization. *Rend. Lincei-Sci. Fis. E Nat.* **2019**, *30*, 735–746. [[CrossRef](#)]
32. Tong, Y.; Cai, Y.; Wang, X.; Li, Z.; Nevin, A.; Ma, Q. Polychrome arhat figures dated from the Song Dynasty (960–1279 CE) at the Lingyan Temple, Changqing, Shandong, China. *Herit. Sci.* **2021**, *9*, 117. [[CrossRef](#)]
33. Li, J.Z.; Zha, J.R.; Pan, X.X.; Zhao, T.; Li, J.F.; Guo, H. A study of Song Dynasty polychrome statue-making techniques and materials in the Sage Mother Hall of the Jinci Temple, Shanxi, China. *Crystals* **2022**, *12*, 1003. [[CrossRef](#)]
34. Wang, F.; Xia, Y.; Liu, J. Analysis of pigments of painted cultural relics unearthed from the burial pits of Han Tombs in Xiangshan, Qingzhou, Shandong. *Emperor Qinshihuang's Mausol. Site Mus.* **2013**, 458–466.
35. Liu, J.-H.; He, Y.; Ke, W.; Hwang, M.-c.; Chen, K.Y. Cinnabar use in Anyang of bronze age China: Study with micro-Raman spectroscopy and X-ray fluorescence. *J. Archaeol. Sci. Rep.* **2022**, *43*, 103460. [[CrossRef](#)]
36. Han, J. External Alchemy and Science of TCM Formula in Song Dynasty. *Stud. Hist. Nat. Sci.* **2008**, *107*, 337–352.
37. Zhu, T.; Chen, J.; Hui, R.; Gong, L.; Zhang, W.-H.; Zhang, Y. Spectroscopic Characterization of the Architectural Painting from the Cizhong Catholic Church of Yunnan Province, China. *Anal. Lett.* **2013**, *46*, 2253–2264. [[CrossRef](#)]
38. van der Weerd, J.; Smith, G.D.; Firtha, S.; Clarka, R.J.H. Identification of black pigments on prehistoric Southwest American potsherds by infrared and Raman microscopy. *J. Archaeol. Sci.* **2004**, *31*, 1429–1437. [[CrossRef](#)]
39. Teri, G.; Fu, P.; Han, K.; Li, J.; Li, Y.; Jia, Z.; Wang, Y.; Li, Y. Color Paintings of Taiping Heavenly Kingdom Royal Residence: An Analytical Study. *Coatings* **2022**, *12*, 1880. [[CrossRef](#)]

40. Schwan, J.; Ulrich, S.; Batori, V.; Ehrhardt, H.; Silva, S.R.P. Raman spectroscopy on amorphous carbon films. *J. Appl. Phys.* **1996**, *80*, 440–447. [[CrossRef](#)]
41. Chenhui, Y. The aesthetic value of black in contemporary oil painting. *Univ. Educ.* **2021**, *137*, 139–142.
42. Tatsch, E.; Schrader, B. Near-infrared Fourier transform Raman spectroscopy of indigoids. *J. Raman Spectrosc.* **1995**, *26*, 467–473. [[CrossRef](#)]
43. Ju, Z.; Sun, J.; Liu, Y.P. Molecular structures and spectral properties of natural indigo and indirubin: Experimental and DFT studies. *Molecules* **2019**, *24*, 3831. [[CrossRef](#)]
44. Tomkinson, J.; Bacci, M.; Picollo, M.; Colognesi, D. The vibrational spectroscopy of indigo: A reassessment. *Vib. Spectrosc.* **2009**, *50*, 268–276. [[CrossRef](#)]
45. Splitstoser, J.C.; Dillehay, T.D.; Wouters, J.; Claro, A. Early pre-Hispanic use of indigo blue in Peru. *Sci. Adv.* **2016**, *2*, e1501623. [[CrossRef](#)]
46. He, Q. Analysis and identification of blue vegetable dyes on a group of ancient silk fabrics. *Sci. Conserv. Archaeol.* **2012**, *24*, 8.
47. de Agredos-Pascual, M.L.V.; Roldan-Garcia, C.; Murcia-Mascaros, S.; Barber, D.J.; Sanchez, M.G.J.; Faugere, B.; Darras, V. Multianalytical characterization of pigments from funerary artefacts belongs to the Chupicuaro Culture (Western Mexico): Oldest Maya blue and cinnabar identified in Pre-Columbian Mesoamerica. *Microchem. J.* **2019**, *150*, 104101. [[CrossRef](#)]
48. Pascual, M.; Carbo, M.T.D.; Carbo, A.D. Characterization of Maya Blue pigment in pre-classic and classic monumental architecture of the ancient pre-Columbian city of Calakmul (Campeche, Mexico). *J. Cult. Herit.* **2011**, *12*, 140–148. [[CrossRef](#)]
49. Ion, R.; Ion, M.; Niculescu, V.; Dumitriu, I.; Fierascu, R.; Florea, G.; Bercu, C.; Serban, S. Spectral analysis of original and restaurated ancient paper from Romanian gospel. *Rom. J. Phys.* **2008**, *53*, 781–791.
50. Tawiah, B.; Asinyo, B.K.; Badoe, W.; Zhang, L.; Fu, S. Phthalocyanine green aluminum pigment prepared by inorganic acid radical/radical polymerization for waterborne textile applications. *Int. J. Ind. Chem.* **2017**, *8*, 17–28. [[CrossRef](#)]
51. Moorthy, J.; Eddington, D.T.; Beebe, D.J. *Microsystem Engineering for Lab-on-a-Chip Devices*. By Oliver Geschke, Henning Klank and Pieter Tellemann. *Angew. Chem. Int. Ed.* **2004**, *116*, 43. [[CrossRef](#)]
52. Zhan, W.; Ling, H.; Tie-bao, Z. Several points about appraising the frescos of the Taiping Heavenly Kingdom. *Southeast Cult.* **2009**, 91–97.
53. Chaplin, T.D.; Clark, R.J.; Singer, B.W. Early 20th C Russian painting? Raman identification of modern pigments on a pastel supposedly Painted by the renowned artist Natalia Goncharova. *J. Raman Spectrosc.* **2014**, *45*, 1322–1325. [[CrossRef](#)]
54. Dallongeville, S.; Garnier, N.; Rolando, C.; Tokarski, C. Proteins in art, archaeology, and paleontology: From detection to identification. *Chem. Rev.* **2016**, *116*, 72–79. [[CrossRef](#)] [[PubMed](#)]
55. Chiavari, G.; Galletti, G.C. Pyrolysis—Gas chromatography/mass spectrometry of amino acids. *J. Anal. Appl. Pyrolysis* **1992**, *24*, 123–137. [[CrossRef](#)]
56. Calvano, C.; Rigante, E.; Picca, R.; Cataldi, T.; Sabbatini, L. An easily transferable protocol for in-situ quasi-non-invasive analysis of protein binders in works of art. *Talanta* **2020**, *215*, 120882. [[CrossRef](#)] [[PubMed](#)]
57. Wang, N.; Zhang, T.; Min, J.; Li, G.; Ding, Y.; Liu, J.; Gu, A.; Kang, B.; Li, Y.; Lei, Y. Analytical investigation into materials and technique: Carved lacquer decorated panel from Fuwangge in the Forbidden City of Qianlong Period, Qing Dynasty. *J. Archaeol. Sci. Rep.* **2018**, *17*, 529–537. [[CrossRef](#)]
58. Wang, N.; He, L.; Zhao, X.; Simon, S. Comparative analysis of eastern and western drying-oil binding media used in polychromic artworks by pyrolysis-gas chromatography/mass spectrometry under the influence of pigments. *Microchem. J.* **2015**, *123*, 201–210. [[CrossRef](#)]
59. He, L.; Chiavari, G. Pyrolysis gas chromatography-mass spectrometry was applied to the analysis of oil adhesives in ancient murals. *J. Xi'an Jiaotong Univ.* **2006**, *40*, 1134–1138.
60. Peifan, Q.; Deqi, Y.; Qi, M.; Aijun, S.; Jingqi, S.; Zengjun, Z.; Jianwe, H. Study and restoration of the Yi Ma Wu Hui layer of the ancient coating on the Putuo Zongcheng Temple. *Int. J. Archit. Herit.* **2021**, *15*, 1707–1721. [[CrossRef](#)]

**Disclaimer/Publisher’s Note:** The statements, opinions and data contained in all publications are solely those of the individual author(s) and contributor(s) and not of MDPI and/or the editor(s). MDPI and/or the editor(s) disclaim responsibility for any injury to people or property resulting from any ideas, methods, instructions or products referred to in the content.